Mateusz DYBKOWSKI[1], Piotr MAJDAŃSKI[2]

Wroclaw University of Science and Technology, Department of Electrical Machines, Drives and Measurements
ul Wybrzeze Wyspianskiego 27, 50-370 Wroclaw, Poland (1,2)
ORCID: 1. 0000-0002-9477-4079; 2. 0000-0002-7427-5766

doi:10.15199/48.2023.05.37

Induction motor stator faults identification using modified MRAS type estimator

***Abstract**. In the paper, the possibility of the MRAS (Model Reference Adaptive System) estimator application to estimate the stator resistance of an induction motor during stator short-circuits is presented. To increase the accuracy of the motor parameter reconstruction, a modified induction motor model was used, taking into account the possibility of simulating short circuits to develop a resistance estimator. The tests were performed in the DTC-SVM vector control system. The simulation results made in Matlab Simulink environment are presented under different drive conditions.*

***Streszczenie.** W artykule przedstawiono możliwość wykorzystania estymatora typu MRAS (Model Reference Adaptive System) do estymacji rezystancji stojana silnika indukcyjnego podczas zwarć zwojowych. W celu zwiększenia dokładności odtwarzania parametru silnika estymator opracowano w oparciu o zmodyfikowany model maszyny, uwzględniający możliwość symulowania zwarć. Badania wykonano w układzie sterowania wektorowego DTC-SVM. Przedstawiono wyniki symulacyjne wykonane w środowisku Matlab Simulink. (**Wykrywanie uszkodzeń stojana silnika indukcyjnego przy wykorzystaniu zmodyfikowanego estymatora typu MRAS**).*

Słowa kluczowe: MRAS, estymacja rezystancji stojana, uszkodzenia stojana, DTC.
Keywords: MRAS, stator resistance estimation, stator faults, DTC.

Introduction

Three-phase asynchronous motors are the most widely used motors in the industry [1]. Along with Permanent Magnet Synchronous Motors (PMSM), Induction Motors (IM) are also increasingly used in Electric Vehicles (EV) and Hybrid Electric Vehicles (HEV) as a consequence of the need to reduce CO2 emissions, lower cost, higher reliability and, easiness of control [2], [3].

To ensure precise control of the angular speed and the electromagnetic torque of the IM, vector control methods are used. Those algorithms require feedback information about certain unmeasurable state variables such as electromagnetic torque, stator flux or rotor flux. There are plenty of methods used to estimate these variables, such as MRAS based estimators [5], [6], Luenberger observers [7], [8], Kalman filter [9], [10], neural network [11], [12]. The accuracy of many of these depends on the correct identification of parameters of the IM equivalent circuit [13], especially those methods based on the mathematical model of the asynchronous machine. During changes in temperature and humidity, the IM parameters change. These may lead to incorrect operation of the estimators and even to loss of drive stability. Motor parameters also change during stator failures (stator resistance) or rotor failures (rotor resistance). Therefore, it is necessary to estimate these parameters in drives with an increased degree of safety.

However, they can also sometimes fail, regardless of their reliability and many other advantages. The most common failures are bearing mechanical failures, the second being short circuits in the stator winding, which account for 25-35% of all failures for medium-voltage motors and up to 65% for high-voltage motors [4]. A phase stator short circuit can damage the machine and stop the industrial process. Inter-turn short circuits progress more slowly, but the consequence of their occurrence is also damage to the machine. Therefore, it is necessary to monitor the condition of the stator windings and turn off the induction machine at the initial stage of failure (one or two shorted turns). On the other hand, it is possible to compensate the stator failures at an early stage of their occurrence. This strategy can be used in the Fault Tolerant Control system (FTC). The MRAS stator resistance estimator can be used for both, diagnostics and compensation.

The article presents a new concept of such a system that uses the induction motor equations that allow modelling of a turn short-circuit. The estimator was verified in the DTC-SVM system under various operating conditions.

Model of the Induction Motor with stator faults

The induction motor model with a modelled faulty stator winding described in [14] was used in this paper to perform the computer simulations. This model allows to simulate Internal Turn Short Circuit (ITSC) in any phase of the motor. Figure 1 shows a simplified schematic diagram of the stator windings with short circuit in phase A. The machine model is described in the stationary reference frame (α-β), using a per unit [p.u.] system.

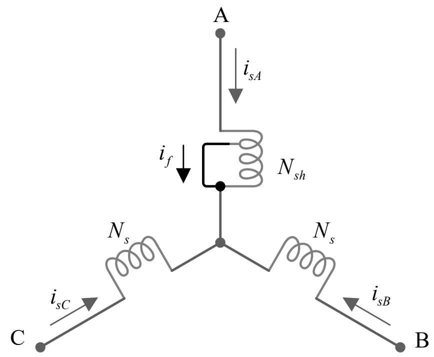

Fig. 1. Scheme of induction motor stator windings with short circuit between turns of phase A

The vector fault $\boldsymbol{\mu}_{\alpha\beta} = \mu_\alpha + j\mu_\beta$ can be defined, where the vector direction represents the phase in which the fault occurs, and the modulus represents the percentage of short-circuited windings.

$$\boldsymbol{\mu}_{\alpha\beta|A} = \eta_A \begin{bmatrix} 1 & 0 \end{bmatrix}^T$$
$$\boldsymbol{\mu}_{\alpha\beta|B} = \eta_B \begin{bmatrix} \frac{-1}{2} & \frac{\sqrt{3}}{2} \end{bmatrix}^T , \quad (1)$$
$$\boldsymbol{\mu}_{\alpha\beta|C} = \eta_C \begin{bmatrix} \frac{-1}{2} & \frac{-\sqrt{3}}{2} \end{bmatrix}^T$$

where $\eta_{A,B,C} = \frac{N_{shA,B,C}}{N_s}$ – fractions of shorted turns in phase A, B, C of stator windings, respectively, N_s – number of turns per phase, N_{sh} – number of shorted turns in phase.

The current in the shorted circuit can be calculated by the following equation:

$$i_f = \frac{\Psi_f - \left(\mu_\alpha \Psi_{s\alpha} + \mu_\beta \Psi_{s\beta}\right)}{\left(\frac{2}{3}\left|\boldsymbol{\mu}_{\boldsymbol{\alpha\beta}}\right|^2 - \left|\boldsymbol{\mu}_{\boldsymbol{\alpha\beta}}\right|\right) x_{\sigma s}}, \tag{2}$$

where Ψ_f – electromagnetic flux in the shorted circuit, $\Psi_{s\alpha}, \Psi_{s\beta}$ – stator fluxes in stationary reference frame, $x_{\sigma s}$ – stator winding leakage inductance.

The electromagnetic flux in the shorted circuit is described by:

$$T_N \frac{\mathrm{d}\Psi_f}{\mathrm{d}t} = -r_s\left(\mu_\alpha i_{s\alpha} + \mu_\beta i_{s\beta}\right) + \left(\left|\boldsymbol{\mu}_{\boldsymbol{\alpha\beta}}\right| r_s + r_f\right) i_f, \tag{3}$$

where $T_N = \frac{1}{2\pi f_{sN}}$ – nominal time constant introduced by the per unit system, f_{sN} – nominal frequency in physical units, r_s – stator winding resistance, $i_{s\alpha}, i_{s\beta}$ – stator currents, r_f – fault resistance, $r_f = 0$ in the case of metallic short circuit.

According to [14], the machine model is expressed by equations:

voltage equations of the stator flux:

$$\begin{aligned} T_N \frac{\mathrm{d}\Psi_{s\alpha}}{\mathrm{d}t} &= u_{s\alpha} - r_s i_{s\alpha} + \frac{2}{3}\mu_\alpha r_s i_f \\ T_N \frac{\mathrm{d}\Psi_{s\beta}}{\mathrm{d}t} &= u_{s\beta} - r_s i_{s\beta} + \frac{2}{3}\mu_\beta r_s i_f \end{aligned}, \tag{4}$$

voltage equations of the rotor flux:

$$\begin{aligned} T_N \frac{\mathrm{d}\Psi_{r\alpha}}{\mathrm{d}t} &= u_{r\alpha} - r_r i_{r\alpha} - \omega_m \Psi_{r\beta} \\ T_N \frac{\mathrm{d}\Psi_{r\beta}}{\mathrm{d}t} &= u_{r\beta} - r_r i_{r\beta} + \omega_m \Psi_{r\alpha} \end{aligned}, \tag{5}$$

flux-current equations:

$$\begin{aligned} i_{s\alpha} &= \frac{x_r}{w}\Psi_{s\alpha} - \frac{x_M}{w}\Psi_{r\alpha} + \frac{2}{3}\mu_\alpha i_f \\ i_{s\beta} &= \frac{x_r}{w}\Psi_{s\beta} - \frac{x_M}{w}\Psi_{r\beta} + \frac{2}{3}\mu_\beta i_f \end{aligned}, \tag{6}$$

$$\begin{aligned} i_{r\alpha} &= \frac{x_s}{w}\Psi_{r\alpha} - \frac{x_M}{w}\Psi_{s\alpha} \\ i_{r\beta} &= \frac{x_s}{w}\Psi_{r\beta} - \frac{x_M}{w}\Psi_{s\beta} \end{aligned}, \tag{7}$$

electromagnetic torque equation:

$$t_E = \Psi_{s\alpha}\left(i_{s\beta} - \frac{2}{3}\mu_\beta i_f\right) - \Psi_{s\beta}\left(i_{s\alpha} - \frac{2}{3}\mu_\alpha i_f\right), \tag{8}$$

mechanical dynamics equation:

$$\frac{\mathrm{d}\omega_m}{\mathrm{d}t} = \frac{1}{T_M}\left(t_E - t_L\right), \tag{9}$$

where $u_{s\alpha}, u_{s\beta}$ – stator voltages, $i_{r\alpha}, i_{r\beta}$ – rotor currents, $\Psi_{r\alpha}, \Psi_{r\beta}$ – rotor electromagnetic fluxes, $u_{r\alpha}, u_{r\beta}$ – rotor voltages, r_r – rotor winding resistance, ω_m – rotor speed, x_r, x_s, x_M – rotor, stator, magnetizing inductances, respectively, $w = x_s x_r - x_M^2$, t_L – load torque, T_M – mechanical time constant.

Control structure of the Induction Motor

Simulations were performed in closed control loops of speed and stator flux with the DTC-SVM control method described in [15]. The scheme of the control structure is shown in figure 2.

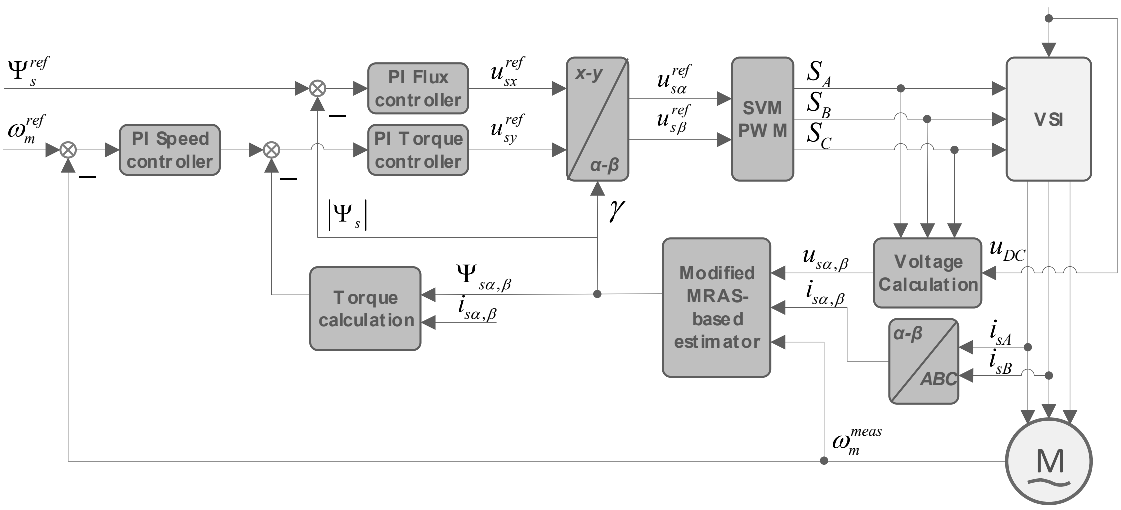

Fig. 2. Schematic diagram of DTC-SVM control structure

Direct Torque Control allows to achieve good dynamic properties and the use of SVM modulator allows to reduce the ripples of torque and flux. The reference frame of this method is oriented with respect to the stator flux.

For the stator flux, two well-known and widely used estimators can be used:

Voltage Model (VM) based on stator voltage equations and flux-current equations of the IM:

$$\begin{aligned} \Psi_{s\alpha}^{VM} &= \int \frac{1}{T_N}\left(u_{s\alpha} - r_s i_{s\alpha}\right)\mathrm{d}t \\ \Psi_{s\beta}^{VM} &= \int \frac{1}{T_N}\left(u_{s\beta} - r_s i_{s\beta}\right)\mathrm{d}t \end{aligned}, \tag{10}$$

$$\begin{aligned} \Psi_{r\alpha}^{VM} &= \frac{x_r}{x_M}(\Psi_{s\alpha}^{VM} - \sigma x_s i_{s\alpha}) \\ \Psi_{r\beta}^{VM} &= \frac{x_r}{x_M}(\Psi_{s\beta}^{VM} - \sigma x_s i_{s\beta}) \end{aligned}, \tag{11}$$

and Current Model (CM) based on rotor voltage equations and flux-current equations of the IM:

$$\begin{aligned}\Psi_{r\alpha}^{CM} &= \int \frac{1}{T_N}\left(\frac{r_r}{x_r}\left(x_M i_{s\alpha} - \Psi_{r\alpha}^{CM}\right) - \omega_m \Psi_{r\beta}^{CM}\right)\mathrm{d}t \\ \Psi_{r\beta}^{CM} &= \int \frac{1}{T_N}\left(\frac{r_r}{x_r}\left(x_M i_{s\beta} - \Psi_{r\beta}^{CM}\right) + \omega_m \Psi_{r\alpha}^{CM}\right)\mathrm{d}t\end{aligned} \quad (12)$$

$$\begin{aligned}\Psi_{s\alpha}^{CM} &= \Psi_{r\alpha}^{CM}\frac{x_M}{x_r} + \sigma x_s i_{s\alpha} \\ \Psi_{s\beta}^{CM} &= \Psi_{r\beta}^{CM}\frac{x_M}{x_r} + \sigma x_s i_{s\beta}\end{aligned} \quad (13)$$

where $\sigma = 1 - \frac{x_M^2}{x_s x_r}$.

Modified MRAS-type estimator

In the case of an ITSC occurrence during motor operation, the basic CM and VM estimators calculate the flux vector components with error, as they are based on the equations of a healthy IM. They are also required information on the unmeasurable parameters of the machine, such as the stator winding resistance. Changes in this parameter can be caused by temperature variations of the machine or by a winding turn fault. In the paper, a modified estimator, robust to these factors is presented.

The modified MRAS estimator (fig. 5) consists of two elements: the relevant stator flux and stator resistance estimator and the additional current estimator. The proper estimator is made up of three subsystems:

- standard Voltage Model (VM) given by (10)-(11) equations, adjusted by the estimated stator resistance r_s^{est} , it calculates the rotor flux Ψ_r^{VM} ;
- modified Current Model, based on (5)-(7) equations, given by:

$$\begin{aligned}\Psi_{r\alpha}^{mCM} &= \int \frac{1}{T_N}\left(\frac{r_r}{x_r}\left(x_M\left(i_{s\alpha} - \frac{2}{3}\mu_\alpha i_f\right) - \Psi_{r\alpha}^{mCM}\right) - \omega_m \Psi_{r\beta}^{mCM}\right)\mathrm{d}t \\ \Psi_{r\beta}^{mCM} &= \int \frac{1}{T_N}\left(\frac{r_r}{x_r}\left(x_M\left(i_{s\beta} - \frac{2}{3}\mu_\beta i_f\right) - \Psi_{r\beta}^{mCM}\right) + \omega_m \Psi_{r\alpha}^{mCM}\right)\mathrm{d}t\end{aligned}, \quad (14)$$

- PI-based Adaptation Mechanism, given by (17), it calculates the stator resistance r_s^{est}.

The difference between the standard CM and the modified one is the presence of the $\frac{2}{3}\boldsymbol{\mu}_{\alpha\beta} i_f$ factor which is impossible to measure. It is directly related with the ITSC and therefore, the modified CM should work properly in the faulted and healthy IM condition, as the value of this factor is zero when no short circuit occurs in stator windings.
The method described in [14] based on the current observer was used to reconstruct the value of this factor. It is based on the assumption that the $\frac{2}{3}\boldsymbol{\mu}_{\alpha\beta} i_f$ factor is not present in the estimated stator current i_s^{est} but it is enclosed in the measured stator current i_s^{meas} . Therefore, the $\frac{2}{3}\boldsymbol{\mu}_{\alpha\beta} i_f$ factor is equal to the difference between these two currents:

$$\frac{2}{3}\boldsymbol{\mu}_{\alpha\beta} i_f = i_s^{meas} - i_s^{est}. \quad (15)$$

On the basis of the equivalent belief, a modified rotor flux estimator was made and described in [16]. The estimated stator current is given by equations which are based on the healthy IM current equations:

$$\begin{aligned}i_{s\alpha}^{est} &= \frac{x_r}{w}\Psi_{s\alpha}^{VM} - \frac{x_M}{w}\Psi_{r\alpha}^{CM} \\ i_{s\beta}^{est} &= \frac{x_r}{w}\Psi_{s\beta}^{VM} - \frac{x_M}{w}\Psi_{r\beta}^{CM}\end{aligned}. \quad (16)$$

where $w = x_s x_r - x_m^2$

Stator fluxes Ψ_s^{VM} and Ψ_r^{CM} are calculated by the Voltage (given by (10)-(11)) and Current Model (given by (12)-(13)) both adjusted by i_s^{est} . The scheme of current estimator is shown in figure 3.

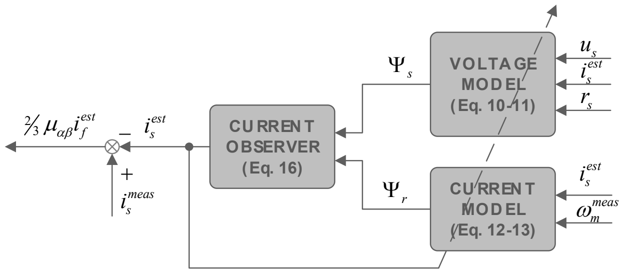

Fig. 3. Schematic diagram of the current estimator

Estimated coefficient $\frac{2}{3}\boldsymbol{\mu}_{\alpha\beta} i_f$ can be used to modify the standard CM and simultaneously make estimation of the rotor flux more accurate when ITSC occurs. The scheme of this kind estimator is presented in figure 4.

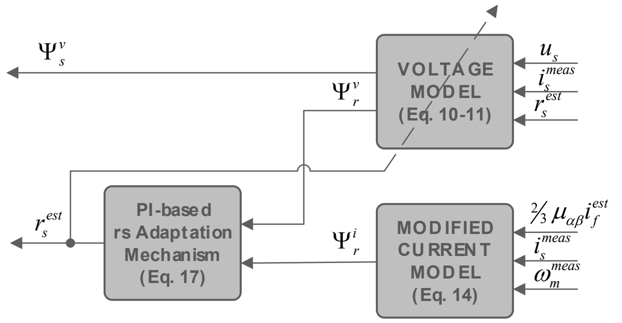

Fig. 4. Schematic diagram of the stator flux and resistance estimator

The PI-based Adaptation Mechanism is used to estimate stator resistance r_s^{est}. It is based on the similar method described in [5]. It is expressed as follows:

$$\begin{aligned}e_{rs} &= i_{s\alpha}(\Psi_{r\alpha}^{VM} - \Psi_{r\alpha}^{CM}) + i_{s\beta}(\Psi_{r\beta}^{VM} - \Psi_{r\beta}^{CM}) \\ r_s^{est} &= K_P^{rs} e_{rs} + K_I^{rs}\int e_{rs}\,\mathrm{d}t\end{aligned}, \quad (17)$$

where K_P^{rs} and K_I^{rs} are PI non-negative coefficients for proportional and integral terms of PI controller. The scheme of the whole modified MRAS-based estimator is shown in figure 5.

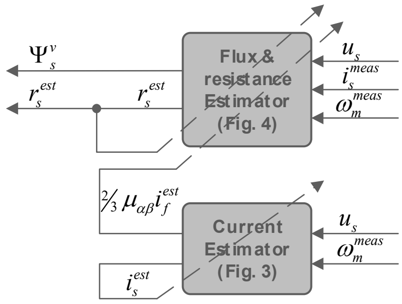

Fig. 5. Schematic diagram of the proposed MRAS-based estimator and the current estimator

Analysis of the novel stator resistance MRAS estimator

This section includes the results of the simulation verification of the MRAS estimator. The estimator was examined for different conditions of the drive operations, such as: load torque and speed variations. The rated data of the tested induction motor are summarized in Table 1 (Appendix A). During the simulation tests, the values of the adaptation mechanism coefficients were the same (Appendix B). State variables of the drive, such as: rotational speed, electromagnetic torque, and stator flux are presented along with the internal signal from the MRAS estimator: estimated stator resistance. Each of the signals and state variables is normalized to its nominal value.

To present the correctness of the estimator's work, it is first necessary to verify the stator current estimation. In figure 6, the simulation results for $\omega^{ref} = 0{,}5\omega_N$ and $T_l = 0{,}5T_N$ are shown.

Only the $\frac{2}{3}\boldsymbol{\mu}_{\alpha\beta} i_f$ coefficient is presented. The actual value comes from the IM model and is a reference point for assessing the correctness of the estimator operation. The estimated value comes from the estimation system (Fig. 3). During the tests, an increase of the stator resistance and a change in the stator resistance caused by a stator short-circuit were assumed.

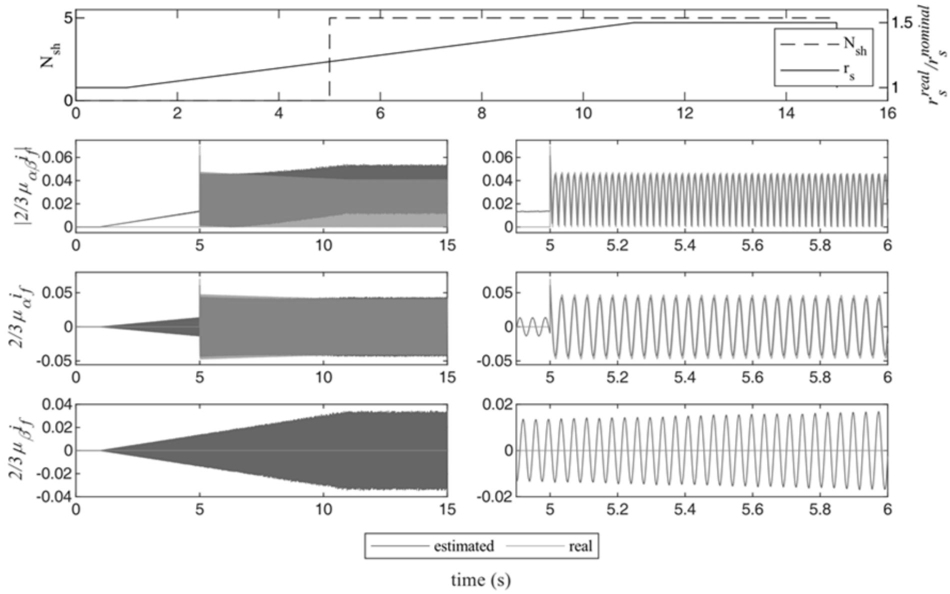

Fig. 6. Operation of the current estimator during increasing stator resistance and short circuit; ($\omega^{ref} = 0{,}5\omega_N$ and $T_l = 0{,}5T_N$)

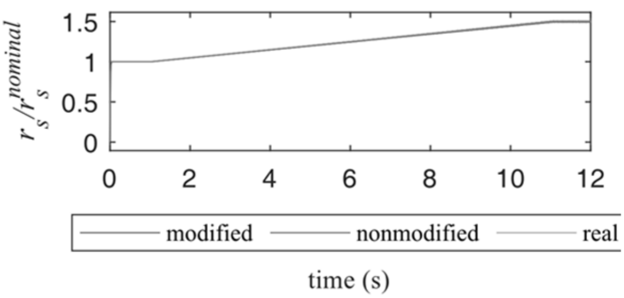

Fig. 7. Operation of the modified and unmodified stator resistance estimator during stator resistance increase; ($\omega^{ref} = \omega_N$ and $T_l = T_N$)

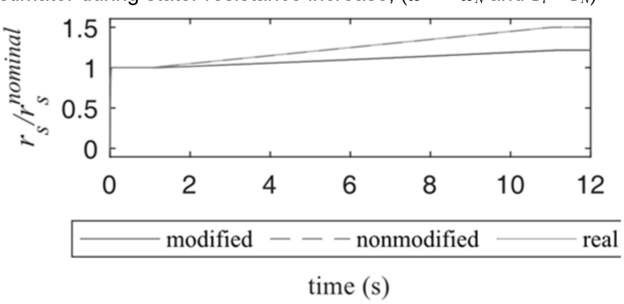

Fig. 8. Operation of modified and unmodified stator resistance estimator during stator resistance increase; ($\omega^{ref} = 0{,}5\omega_N$ and $T_l = 0{,}5T_N$)

It can be easily observed that as the stator resistance increases, the fault current i_f appears in both axes. Hence, it can be concluded that this observer is not robust to changes in stator resistance. This is because the voltage and current models are based on the classical induction motor model.

Figures 7 and 8 show the results of the stator resistance estimation using the standard, unmodified MRAS [5] and the estimator modified by the $\frac{2}{3}\boldsymbol{\mu}_{\alpha\beta} i_f$ coefficient.

Under full load conditions and operation at rated speed, these estimators operate identically correctly (fig. 7) but there is a noticeable difference under $\omega^{ref} = 0{,}5\omega_N$ and $T_l = 0{,}5T_N$ conditions.

The effect of the load torque on the operation of the estimator with the motor operating at rated speed was studied and the results are shown in figure 9. In 0-3 s time $T_l = T_N$; in 3-5s time $T_l = 0{,}75T_N$; in 5-7s time $T_l = 0{,}5T_N$; in 7-10s time $T_l = 0{,}25T_N$; in 10-12s time there is no load.

The results show that changes in torque load impact the performance of the modified with the $\frac{2}{3}\boldsymbol{\mu}_{\alpha\beta} i_f$ coefficient MRAS estimator.

In figure 10, the comparison of operation of the proposed estimator with the traditional one during stator fault condition is shown. The short circuit of N_{sh} = 1, 2, 3, 5 and 8 are simulated at the time t = 3s, 6s, 9s, 12s, 15s, respectively.

Analyzing the obtained results, it can be seen that the estimated value of the stator resistance decreases with the number of shorted coils. In the traditional MRAS model, these decreases are more significant and the estimated resistance value rapidly reaches unrealistic negative values. It may suggest that this estimator is more suited to fault identification but is not suitable for fault compensation by adjusting the Voltage Model with an estimated stator resistance value. In the modified model, the resistance changes are smaller and therefore this possible application was tested and the results are shown in figure 11.

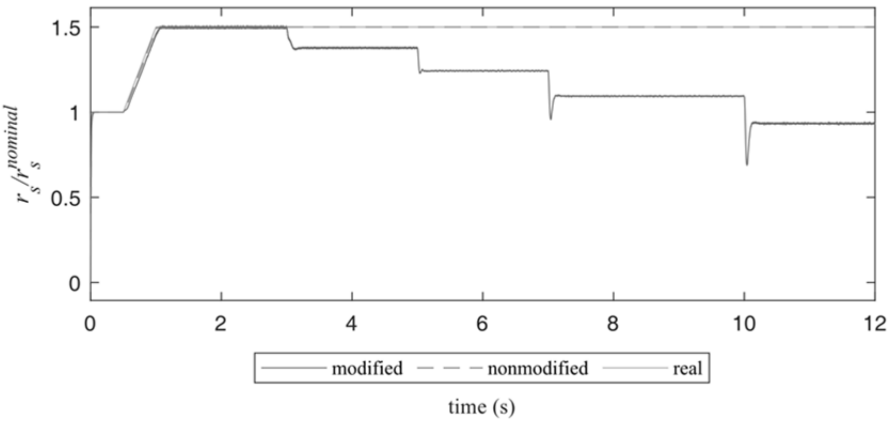

Fig. 9. Operation of the modified stator resistance estimator during stator resistance increase and load torque changing; ($\omega^{ref} = \omega_N$)

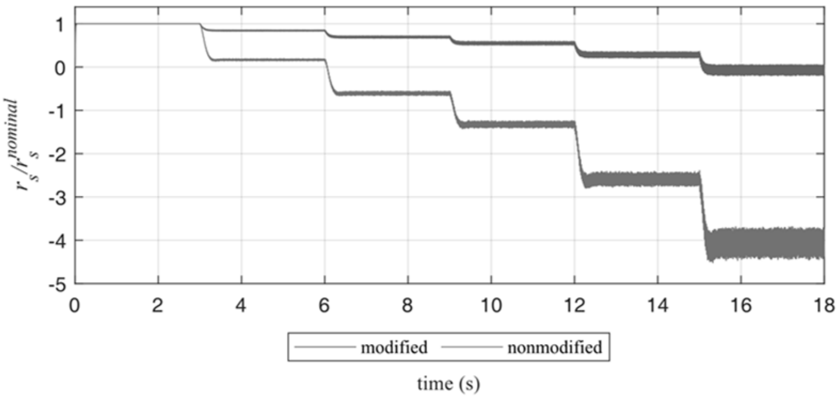

Fig. 10. Comparison of the operation of the modified and unmodified stator resistance estimator during the intern-turn short circuit; ($\omega^{ref} = 0{,}5\omega_N$ and $T_l = 0{,}5T_N$)

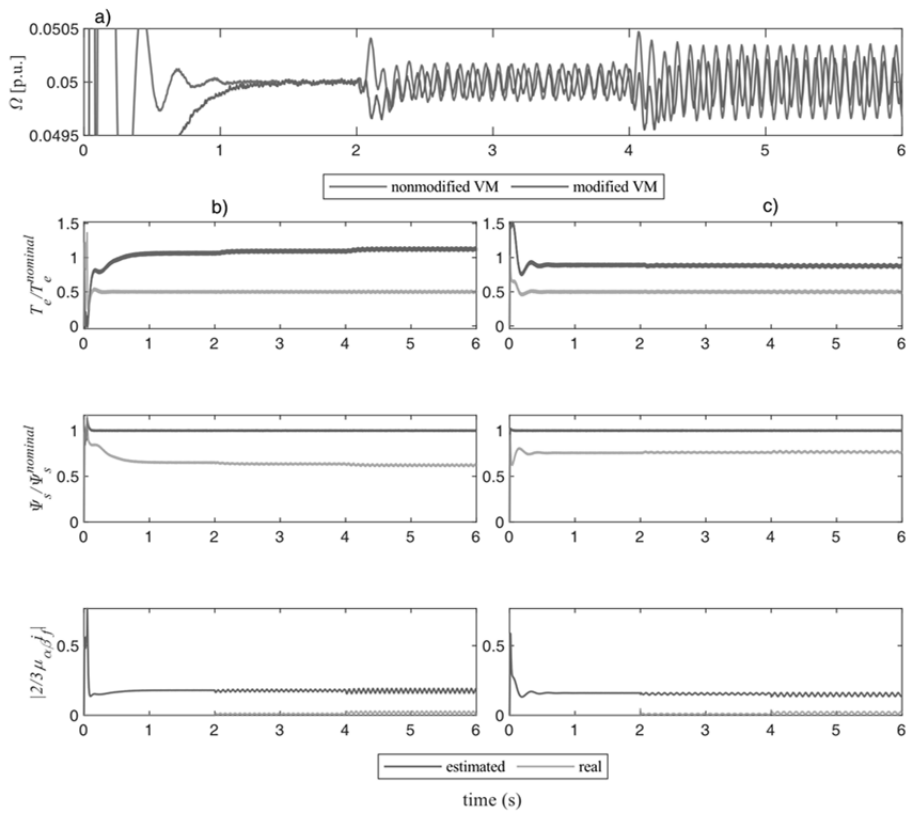

Fig. 11. Comparison of the operation of the induction motor working in a DTC-SVM closed-loop structure with the modified (adjusted by stator resistance) and classical Voltage Model as a flux estimator during the intern-turn short circuit; ($\omega^{ref} = 0{,}05\omega_N$, $T_l = 0{,}5T_N$ and $r_s = 1{,}5r_{sN}$): a) speed b) electromagnetic torque, stator flux and fault current from model with unmodified VM compared to real values, c) electromagnetic torque, stator flux and fault current from model with modified VM compared to real values.

Simulations were carried out under the conditions of $\omega^{ref} = 0{,}05\omega_N$, $T_l = 0{,}5T_N$ with an unmodified Voltage Model and with the Voltage Model adjusted by the estimated stator resistance. In t = 2s shorts of 5 (1,3%) coils and in t = 4s shorts of 10 (2,6%) coils were simulated.

Figure 11a shows a comparison of the motor speed operating in the DTCSVM system with the modified and unmodified VM. It can be seen that with the occurrence of short circuits the speed begins to oscillate and that these oscillations are smaller in the system with the modified estimator. Figures 11b and 11c show the performance of the modified and unmodified Voltage Model. It can be seen that in both cases the estimated values of stator flux and electromagnetic torque are incorrect. The same is true of the short-circuit current, in both systems the current is estimated with too large a value.

Conclusions

The paper presents a modified stator flux and stator resistance estimator, which may have potential application in FTC systems. Its operation was checked in the DTCSVM control system.

It can be seen that the proposed estimator is sensitive to stator damage, but too many state variables, which are tunable, cause incorrect flux estimation.

Therefore, it seems that a better solution for FTC systems is the system described in the earlier work [16], in which the estimator was based not on classical voltage and current models, but on modified equations.

Appendix A

Table 1. Motor parameters

Name	Symbol	Unit	Value
Power	P_N	W	1100
Stator phase voltage	U_{sN}	V	220
Stator current	I_{sN}	A	2,9
Mechanical speed	Ω_N	rpm	1400
Torque	T_N	Nm	7.5030
Frequency	f_N	Hz	50
Stator resistance	r_s	Ω	5.9
Rotor resistance	r_r	Ω	4.559
Stator inductance	x_s	mH	131.1
Rotor inductance	x_r	mH	131.1
Magnetizing inductance	x_M	mH	123.3
Pole pairs	p_b	-	2
Turn per phase	N_s	-	312

Appendix B

Table 2. Adaptation mechanism coefficients

Name	Value
K_P^{rs}	15
K_I^{rs}	15 000

***Authors**: mgr inż. Piotr Majdański, dr hab. inż. Mateusz Dybkowski, Wroclaw University of Science and Technology, Department of Electrical Machines, Drives and Measurements, ul. Wybrzeze Wyspianskiego 27, 50-370 Wrocław, E-mail: piotr.majdanski@pwr.edu.pl, mateusz.dybkowski@pwr.edu.pl;*
ORCID: 1. 0000-0002-7427-5766; 2. 0000-0002-9477-4079

REFERENCES

[1] P. Waide and C. U. Brunner, "Energy-Efficiency Policy Opportunities for Electric Motor-Driven Systems," OECD, Paris, May 2011. doi: 10.1787/5kgg52gb9gjd-en.
[2] A. M. Bazzi, "Electric machines and energy storage technologies in EVs and HEVs for over a century," in 2013 International Electric Machines Drives Conference, May 2013, pp. 212–219. doi: 10.1109/IEMDC.2013.6556255.
[3] P. H. Camargos and R. E. Caetano, "A performance study of a high-torque induction motor designed for light electric vehicles applications," Electr Eng, Jun. 2021, doi: 10.1007/s00202-021-01331-4.
[4] P. Zhang, Y. Du, T. G. Habetler, and B. Lu, "A Survey of Condition Monitoring and Protection Methods for Medium-Voltage Induction Motors," IEEE Transactions on Industry Applications, vol. 47, no. 1, pp. 34–46, Jan. 2011, doi: 10.1109/TIA.2010.2090839.
[5] V. Vasic, S. N. Vukosavic, and E. Levi, "A stator resistance estimation scheme for speed sensorless rotor flux oriented induction motor drives," IEEE Transactions on Energy Conversion, vol. 18, no. 4, pp. 476–483, Dec. 2003, doi: 10.1109/TEC.2003.816595.
[6] M. H. Holakooie, M. Ojaghi, and A. Taheri, "Direct Torque Control of Six-Phase Induction Motor With a Novel MRAS-Based Stator Resistance Estimator," IEEE Transactions on Industrial Electronics, vol. 65, no. 10, pp. 7685–7696, Oct. 2018, doi: 10.1109/TIE.2018.2807410.
[7] S. M. N. Hasan and I. Husain, "A Luenberger–Sliding Mode Observer for Online Parameter Estimation and Adaptation in High-Performance Induction Motor Drives," IEEE Transactions on Industry Applications, vol. 45, no. 2, pp. 772–781, Mar. 2009, doi: 10.1109/TIA.2009.2013602.
[8] M. Jouili, Y. Agrebi, Y. Koubaa, and M. Boussak, "A Luenberger state observer for simultaneous estimation of speed and stator resistance in sensorless IRFOC induction motor drives," in 2015 16th International Conference on Sciences and Techniques of Automatic Control and Computer Engineering (STA), Dec. 2015, pp. 898–904. doi: 10.1109/STA.2015.7505225.
[9] M. A. Usta, H. I. Okumus, and H. Kahveci, "A simplified three-level SVM-DTC induction motor drive with speed and stator resistance estimation based on extended Kalman filter," Electr Eng, vol. 99, no. 2, pp. 707–720, Jun. 2017, doi: 10.1007/s00202-016-0442-x.
[10] Yildiz, M. Barut, E. Zerdali, R. Inan, and R. Demir, "Load torque and stator resistance estimations with unscented Kalman filter for speed-sensorless control of induction motors," in 2017 International Conference on Optimization of Electrical and Electronic Equipment (OPTIM) & 2017 Intl Aegean Conference on Electrical Machines and Power Electronics (ACEMP), May 2017, pp. 456–461. doi: 10.1109/OPTIM.2017.7975011.
[11] B. Karanayil, M. F. Rahman, and C. Grantham, "Online Stator and Rotor Resistance Estimation Scheme Using Artificial Neural Networks for Vector Controlled Speed Sensorless Induction Motor Drive," IEEE Transactions on Industrial Electronics, vol. 54, no. 1, pp. 167–176, Feb. 2007, doi: 10.1109/TIE.2006.888778.
[12] T. Pham Van, D. Vo Tien, Z. Leonowicz, M. Jasinski, T. Sikorski, and P. Chakrabarti, "Online Rotor and Stator Resistance Estimation Based on Artificial Neural Network Applied in Sensorless Induction Motor Drive," Energies, vol. 13, no. 18, Art. no. 18, Jan. 2020, doi: 10.3390/en13184946.
[13] K. Klimkowski, M. Dybkowski, and S. A. Bednarz, "Influence of stator and rotor resistances changes to the properties of the Fault Tolerant Vector Control of induction motor drive," in 2017 International Symposium on Electrical Machines (SME), Jun. 2017, pp. 1–5. doi: 10.1109/ISEM.2017.7993540.
[14] C. H. D. Angelo, G. R. Bossio, S. J. Giaccone, M. I. Valla, J. A. Solsona, and G. O. Garcia, "Online Model-Based Stator-Fault Detection and Identification in Induction Motors," IEEE Transactions on Industrial Electronics, vol. 56, no. 11, pp. 4671–4680, Nov. 2009, doi: 10.1109/TIE.2009.2012468.
[15] C. Lascu, I. Boldea, and F. Blaabjerg, "A modified direct torque control for induction motor sensorless drive," IEEE Transactions on Industry Applications, vol. 36, no. 1, pp. 122–130, Jan. 2000, doi: 10.1109/28.821806.
[16] M. Dybkowski and S. A. Bednarz, "Modified Rotor Flux Estimators for Stator-Fault-Tolerant Vector Controlled Induction Motor Drives," Energies, vol. 12, no. 17, Art. no. 17, Jan. 2019, doi: 10.3390/en12173232.